RESEARCH ARTICLE

Editorial Process: Submission:03/01/2024 Acceptance:06/16/2024

Accuracy of Beamscan Software in Determining the Inflection Point from the FFF Beam Profile Using Several Array Detectors

Kanakavel Kandasamy, E James Jebaseelan Samuel*

Abstract

Objective: The goal of this study is to determine the accuracy of the PTW Beamscan program in determining the inflection point from Flattening Filter Free Beam Profile utilizing Multiple Detectors. **Methods:** True Beam Linear Accelerator with 6FFF and 10FFF Photon Energies and 10 cm, 15 cm and 20 cm Field Sizes were used for this study. Profile measurements were taken with PTW's 729, 1,500, and 1,600 and the Starcheck system, the Pinpoint 3D with Beamscan system, and Linac's EPID. The first-order derivative was utilized in both the Excel spreadsheet and Beamscan software to analyse raw measured data to locate inflection point and the FWHM was calculated. The accuracy of inflection points and FWHM between the Excel sheet calculation and the software program were investigated. **Results:** For 10X10 cm^2 in the 729 Array, the greatest differences in FWHM were 5.16 mm and 5.04 mm for the X6 FFF and X10 FFF Energies, respectively. The largest difference was 2.26 mm for 1,600 SRS arrays with a 15×15 cm^2 field size. The difference in FWHM between Manual and software analysis for 10X10 cm^2 and 20X20 cm^2 Field Sizes is in decreasing order for detectors from 729, 1,500, 1,600 SRS, Starcheck, Pinpoint 3D, and EPID. In contrast, there is no climbing or declining pattern detected in the difference in Field Width for the 15×15 cm^2 Field Size. Similarly, for all detectors except the 1,600 SRS array, the peak of the first-order derivative occurs at the chamber position for a 15X15 cm^2 field size. **Conclusion:** The higher resolution of measurement yields more accuracy in inflection point and the FWHM. Irrespective of measurement resolution, the Beamscan software provided the FWHM closer to the respective nominal Field Size. Out of all detectors, results obtained with Excel Starcheck and EPID are good in agreement with values obtained by the software analysis. Thus, it is shown that Beamscan software is so accurate in determining inflection point of a FFF beam profile and used for routine profile analysis.

Keywords: FFF profile analysis- EPID- starcheck- 1,600 SRS- 729 and 1,500 Array

Asian Pac J Cancer Prev, **25 (6)**, 2177-2184

Introduction

FFF beams have emerged as the treatment of choice for latest and Fast Treatment technique due to their brief treatment delivery time and the fact that the dose rate increases by a factor of two to four when the flattening filter is removed. FFF beams are especially advantageous for SRS and SBRT, but their increased intensity may be applicable to a variety of fields and treatments. The elimination of a flattening filter increases the dose rate and decreases the mean energy, head leakage, and lateral scattering, all of which have been demonstrated to be beneficial in specialized treatment procedures [1,2]. The absence of beam hardening effects results from the transformation of a beam into an FFF beam upon removal of the flattening filter. Once more dependent on the field size, the percentage depth dose pattern has been marginally diminished by the virgin bremsstrahlung beam. These causes for two reasons: (I) an increase in dose/pulse-induced photon energy fluence for FFF beams; (II) off-axis spectra that are not significantly different from those of the central axis for the FFF beam as opposed to a substantial shift in spectrum caused by the insertion of the flattening filter. By comparing the intensity patterns of various linear accelerators with regard to nominal field sizes and inhomogeneity patterns, the intensity of the FFF beam is determined. When calculating the penumbral widths of unflattened beams, the spatial distance between of 80% to 20% isodose lines that was previously applied to conventional beams is no longer applicable. Because the intensity of the FFF Beam differs with lateral distance and shapes gets changed [3]. In general, detectors that were favoured for measurements on ordinary flattened Linac beams were either less suitable for FFF beams or required modifications [4]. Commercially different ionization chambers (Semiflex, Semiflex three dimensional [3D], and Microion chambers), different types of shielded and unshielded diodes, and special detectors – microdiamond are available in the industry for absolute and relative dose measurements. However, there is no ideal detector that satisfies all dosimetric properties from tiny to big fields. In case of diodes, despite their tiny dimensions and great

*Department of Physics, School of Advanced Sciences, VIT University, Vellore, India. *For Correspondence: ejames@vit.ac.in*

sensitivity, diode detectors are not totally ideal due to their energy dependence at low energies and overresponse of shielded diodes (due to the high Z shield). However, for the ion chambers, because of the volume averaging effect and low air density, tiny volume ion chambers are less dependent on photon beam energy than diodes but are less appropriate for small field dosimetry. Another option is a microdiamond detector, which has qualities such as radiation hardness, near tissue equivalence, compact size, and independence from radiation quality [5]. To perform dosimetric measurements for acceptance of FFF Beams and followed by Beam data, various detectors and phantoms were used and studied [6]. To address this challenge, in numerous studies, distinct approaches for FFF Beam analysis were exhibited. In which different methods to perform inflection point analysis have been studied and discussed [7-11]. In these studies, Inflection Point was defined as a point at which physical field size occurs. Fogliata et al. established that the derivative method is among the straightforward and precise techniques utilized to analyse the profiles of unflatten beams [12]. G. Sahani et al. [13] have studied and established that the more practical approach to derive and analyse FFF beam parameters and the inflection point analysis for unflatten beam profiles were done by manual analysis using tangential curve method [13]. PTW has recently launched a software module that analyses inflection points for FFF beam profiles using the first-order derivative method. There is no study on its accuracy in finding inflection point as such. In this work we aimed to use different detector arrays having various resolution to find the accuracy of the software. Numerous previous studies, octavius Modals: 729, 1500, 1600 and Starcheck arrays (PTW Freiburg) and linac EPID panel having different detector resolutions have been used for profile measurement only for flattened beam but not for unflatten Beam [14-19].

Hence, as a pioneer work, using above array detectors, this study sought to assess the precision of the software module in locating inflection points and deducing the full width half maximum of an unflatten beam profile.

Materials and Methods

Materials

Linear Accelerator

Essential measurements were conducted using a TrueBeam™ system (Varian Medical System Palo Alto) [20], which is a high-end modal linear accelerator. This system featured both a flattened and unflattened beam. The photon energies of Linac are X6, X6FFF, X10, X15, and X10FFF. Field sizes ranging from 5x5 mm^2 to 40x40 cm2 are incorporated into the Linac. The maximal dose rates utilized in Linac are as follows: 600 MU/min for FF Beam Energies, 1,600 MU/min for X6FFF Beam Energies, and 2,400 MU/min for X10FFF Beam Energies. In this investigation, only X6FFF and X10FFF photon beams with higher dose rates were utilized.

Measuring Tools

In this investigation, Octavius Detectors - 729, 1,500, and 1,600 SRS, as well as Starcheck (all from PTW Freiburg), were employed [21,22]. Varian's amorphous silicon DMI, i.e., EPID with portal dosimetry, was used to compare these arrays. A Pinpoint 3D chamber (Modal: T31022) was also used to measure the profile along the PTW Beamscan 3D RFA System, which is usually considered a standard and conventional measurement [23,24]. Table 1 lists all measurement instruments and their parameters. Figure 1 depicts a visual representation of the resolution of several array systems. To place detector arrays in their reference point of measurement, a real water (RW3) slab phantom (white dense polystyrene material = 1.045 g/cm^3) with a thickness of 1 cm, a 2 cm chamber, and 1 mm and 2 mm plates was utilized [25]. At appropriate locations, PTW Verisoft software [26], Beamscan Software [27] having Scan Data, and the Image Analysis module were used to measure and extract beam profiles.

Methods

Measurement Setup

Only X6FFF and X10FFF energies, as well as 10X10 cm^2, 15X15 cm^2, and 20X20 cm^2, were employed in this investigation. The output and beam profiles were adjusted in accordance with the international standards IAEA TRS 398 [28] and IEC 60976 [29] prior to the measurement. For precise configuration, all PTW 2D arrays and their effective point of depth (as listed in Table 1) were maintained at a depth of 5 cm using RW3 slabs while considering four numbers of 1 cm, one 1 mm and two 2 mm plates. Backscatter of 10 cm slabs were used behind the array systems. To enhance the scattering from the posterior side of the array, 10-centimeter slabs were positioned. The parameters selected for the common beam were 10x10 cm2, 15x15 cm^2, and 20x20 cm^2, with an SAD of 100 cm. Each array was irradiated with 100 MUs. Whereas the DMI panel was transported to the Linac Isocentre point, SAD, and delivered with the same 100 MU. The imaging files resulting from the irradiation process were saved in DICOM format which were transported to Beamscan' s Film and Image Analysis software . Profiles were then created by utilizing Beamscan' s Film and Image Analysis software. In contrast, the Pinpoint 3D chamber was kept at a depth of 5 cm using a Beamscan system SSD measuring 95 cm. The profiles were scanned for each field size for both energies, and data were extracted. In contrast to the other detectors, the 1600 SRS array was configured with the primary axis of 20x20 cm^2 aligned with the diagonal axis of the array, thereby adhering to the field size restriction of 15x15 cm^2. A measurement was subsequently obtained. To make this study simple, only Inline axis profiles of each detector were considered. To ensure high reproducibility, all arrays and the Pinpoint 3D Chamber were preirradiated with 2 Gy and zeroed prior to delivery. But for EPID Panel alone, image and dosimetric calibration was conducted in accordance with the vendor's guidelines [30].

Inflection Point and FWHM

The point of inflection was determined by taking the first derivative at which the greatest dose difference

Table 1. Technical Specification of Different Detector Arrays

Detector Modal	Detector type	Technical details
Octavius 729	Vented Ion Chamber	Chamber Volume and Nos: 0.125 cc & 729
		Field Size Coverage: 2X2 cm^2 to 27X27 cm2
		Resolution of the array: 10 mm
		Dose Rate range: 3 to 48 Gy/min
		Energy Range: (Co ... 25) MV
		Effective Point of Depth: 7.5 mm from Surface
Octavius 1500	Vented Ion Chamber	Chamber Volume and Nos: 0.06 cc & 1405
		Field Size Coverage: 2X2 cm^2 to 27X27 cm^2
		Resolution of the array: 7.07 mm(Diagonal Axis)
		Dose Rate range: 3 to 48 Gy/min
		Energy Range: (Co ... 25) MV
		Effective Point of Depth: 7.5 mm from Surface
[a]Octavius 1600 SRS	Liquid Filled Ion Chamber	Chamber Volume and Nos: 0.003 cc & 1521
		Field Size Coverage: 1X1 cm^2 to 15X15 cm^2
		Resolution of the array: 5 mm (> 6.5X6.5 cm^2)
		Dose Rate range: 0.8 to 24 Gy/min
		Energy Range: (Co ... 25) MV
		Effective Point of Depth: 9 mm from Surface
Starcheck	Vented Ion Chamber	Chamber Volume and Nos: 0.05cc & 527
		Field Size Coverage: 4X4 cm^2 to 26X26 cm^2
		Resolution of the array: 3 mm
		Dose Rate range: 2 to 80 Gy/min
		Energy Range: (Co... 25) MV
		Effective Point of Depth: 8.5 mm from Surface
Pinpoint 3D (T31022)	Vented Ion Chamber	Volume: 0.016 cc
		Energy Range: Co ... 25 MV photons
		Measurement Resolution: 1 mm
		Field size: 2 x 2 cm^2 to 40 x 40 cm^2
		Max Dose Rate: 91.6 Gy/s
Varian EPID (DMI)	Amorphous Silicon detector	Field Size Coverage: up to 43X43 cm^2
		Resolution: 0.3 mm
		Energy Range: (Co... 25) MV
		Effective Point of Depth: 8.5 mm from Surface

[a], The measuring length at the diagonal axis of the 1600 SRS array is 21 cm; SRS, Stereotactic Radio Surgery; EPID - Electronic Portal Imaging Device; DMI, Digital Megavolt Imager; MV, Mega Voltage

occurred on both extremes of the profile. Furthermore, the distance between the left and right inflection points of the profiles was calculated and termed the FWHM (depicted in Figure 2) [13].

Manual Analysis (Raw Data)

The measured profile was utilized to extract the measured dosages of each array, which were subsequently employed for manual analysis. The first-order derivatives were computed for each dataset obtained from every profile. The mathematical formula provided below was employed to compute the first-order derivatives for each dataset [31]. The formula was utilized within the Microsoft Excel software application to compute the inflection point.

$dy/dx = \Delta y/\Delta x$……………………. (1) [31]

Here dy/dx – First derivative of the measured sample Δy – change in y and Δx – change in x

where x is the distance across the profile in mm and y is the relative dose of a measured profile as a percentage.

Software Analysis

The measured field size was computed by Beamscan software [32] using inflection point data samples from all instruments. By means of linear interpolation, the software augments the existing measuring points with new data points to obtain equidistant data points. Following this, the curve is smoothed. Although the penumbra is obscured by the smoothing operation, its impact on the X-values of the inflection points (position) is minimal. It is possible to compute the first derivative of the smoothed

Table 2. Measured FWHM by All Detectors for the 6FFF Beam.

	10X10 cm^2		15X15 cm^2		20X20 cm^2	
	Manual Analysis (mm)	BS Software (mm)	Manual Analysis (mm)	BS Software (mm)	Manual Analysis (mm)	BS Software (mm)
Array 729	94.00	99.16	150.00	149.91	196.00	199.40
Array 1500	103.50	99.43	148.50	148.55	203.20	199.66
Array 1600	95.50	99.56	148.50	149.83	203.30	200.47
Starcheck	99.00	99.72	150.00	149.67	201.00	199.45
PP3D	100.50	99.71	150.50	149.81	201.00	199.91
EPID	99.60	99.53	150.15	149.82	200.10	200.04

FWHM, Full Width Half Maximum; FFF, Flattening Filter Free; PP3D, Pinpoint 3D; EPID, Electronic Portal Imaging Device; BS, Beamscan Software; mm, milli meter

trajectory. The process of locating the global maximum of the first derivative utilizes brute force. To mitigate the influence of noise, all adjacent points to this maximum are taken into account if their weighted average of X-values exceeds a specified threshold (e.g., half the maximum). The coordinates (X-values) of the inflection points on the left and right are ascertained. By linear interpolation, the corresponding Y-values are derived from the original curve; however, the Y-values of the left and right inflection points may not be identical. The two Y-values are subsequently averaged. Through the process of linear interpolation, the X-values (positions) are adjusted to match the averaged Y-value. FWHMs are ultimately deduced.

Results

The measured profiles are presented for two different energies and three distinct field sizes in Figures (3a, 3b, 4a, 4b, 5a and 5b). The manual analysis approach was used to generate suitable curves for the first-order derivative with regard to distance. These curves are depicted in Supplementary Figures 6 (a...f), 7 (a...f), 8 (a...f), 9 (a...f), 10 (a...f), and 11 (a...f) for X6FFF and X10FFF Photon Beams for Field Sizes 10X10 cm^2, 15X15 cm^2 and 20X20 cm^2 respectively. The FWHM values of the manual analysis were obtained by determining the inflection points using an Excel spreadsheet and analysing the resulting curves. In a similar manner, the FWHM values of the software analysis were derived from the obtained data. The FWHM values were recorded and subsequently compared in Tables 2 and 3. The results presented in supplementary Figures (12 a and b) and Tables 4 and 5 demonstrate the difference in FWHM values obtained from manual analysis and software calculations for both energies. The decreasing order of the difference in field width between manual and software analysis is observed for detectors including 729, 1,500, 1,600 SRS, Starcheck, Pinpoint, and EPID, for field sizes of 10X10 cm^2 and 20X20 cm^2. In the case of 15×15 cm^2 field size,

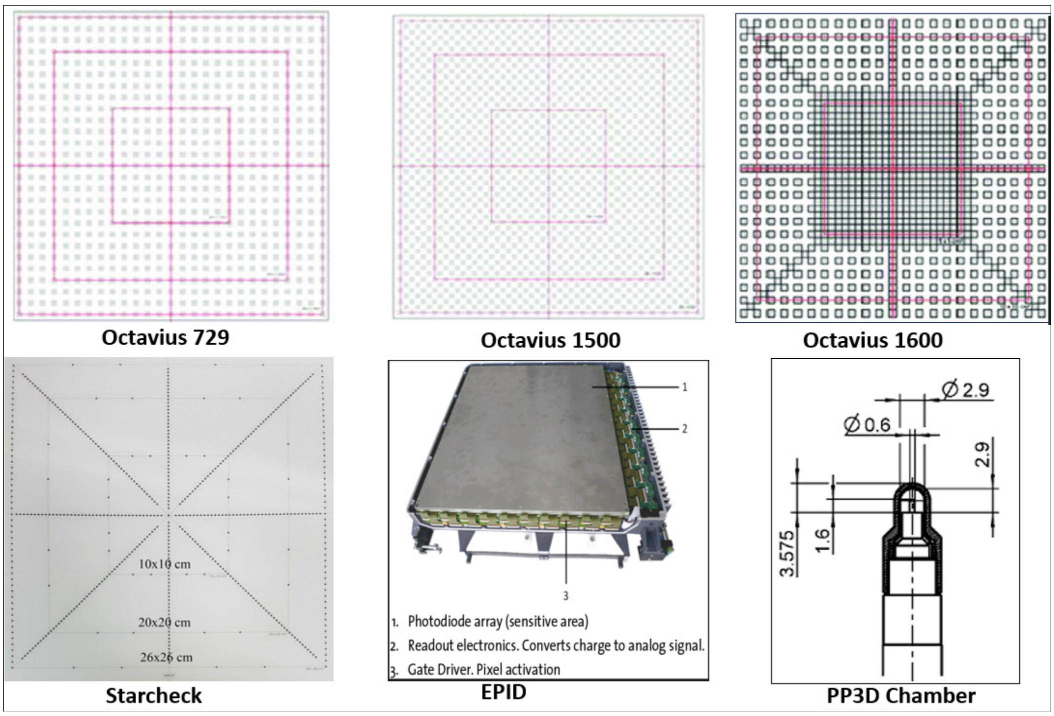

Figure 1. Shows the Individual Array and Its Detector Resolution Pattern. EPID, Electronic Portal Imaging Device; PP3D, Pinpoint 3D

Table 3. Measured FWHM by All Detectors for the 10FFF Beam.

	10X10 cm^2		15X15 cm^2		20X20 cm^2	
	Manual Analysis (mm)	BS Software (mm)	Manual Analysis (mm)	BS Software (mm)	Manual Analysis (mm)	BS Software (mm)
Array 729	93.90	98.92	150.00	149.86	194.50	199.16
Array 1500	103.00	99.22	148.50	148.55	202.90	199.35
Array 1600	97.50	99.53	147.50	149.76	203.00	200.31
Starcheck	99.00	99.67	149.30	149.55	201.00	199.25
PP3D	100.00	99.61	149.50	149.65	200.00	199.76
EPID	99.60	99.44	149.70	149.75	200.10	199.92

FWHM, Full Width Half Maximum; FFF, Flattening Filter Free; PP3D, Pinpoint 3D; EPID, Electronic Portal Imaging Device; BS, Beamscan Software; mm, milli meter

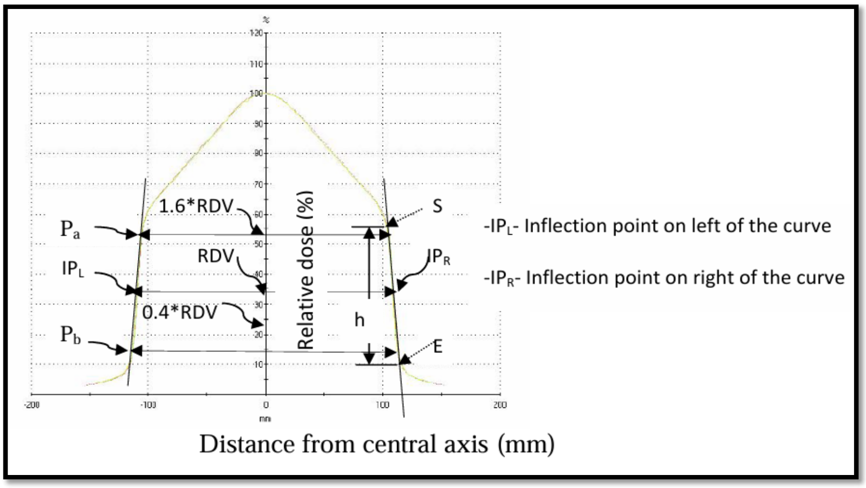

Figure 2. Schematic Diagram for Determining Inflection Point. IP, inflection point; RDV, Reference Dose Value

the similar trend was not observed, and the less difference was noticed in field width. The given figures demonstrate that the peak of the first-order derivative did not occur in any of the chambers inside the 729 and 1,500 arrays, particularly for field sizes of 10X10 cm^2 and 20X20 cm^2. An identical outcome was observed in the 1,600 SRS array when utilizing a 15×15 cm^2 field size. However, this was not the case for Starcheck, Pinpoint 3D, and EPID. In a similar vein, it can be observed that the peak of the first order derivative is consistently located at the chamber position for all detectors, with the exception of the 1,600 SRS array, when considering a field size of 15×15 cm^2. The greatest difference was noted in the 729 arrays for dimensions of 10×10 cm^2 and 20×20 cm^2, measuring 5.16 mm and 3.40 mm, respectively, for X6FFF and that of 5.02 mm and 4.66 mm were recorded for the X10 FFF.

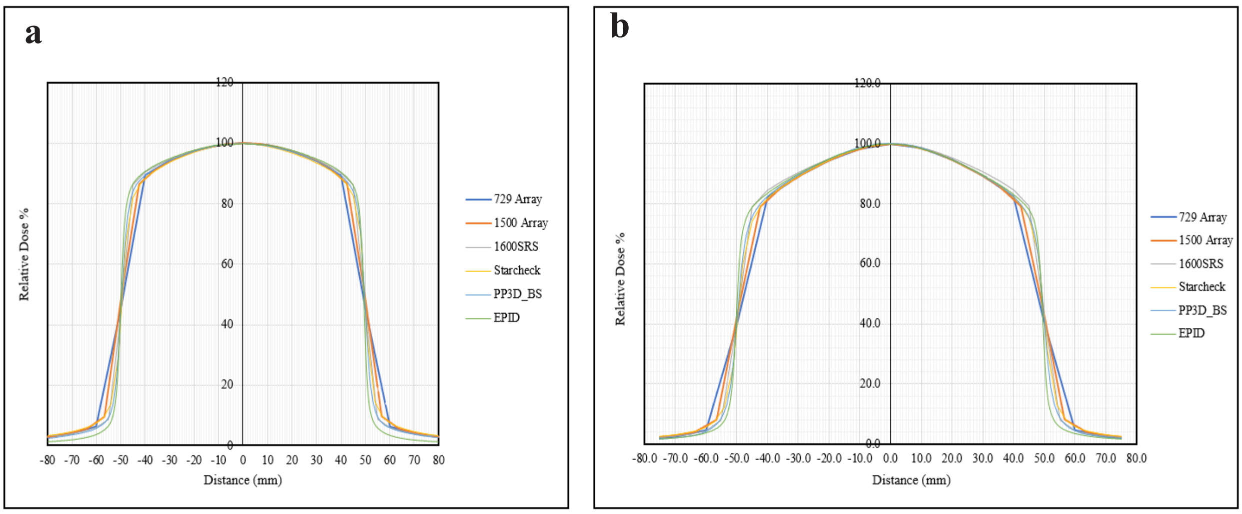

Figure 3. a, 6FFF_10X10 cm^2 Profiles; b, 10FFF_10X10 cm^2 Profiles. EPID, Electronic Portal Imaging Device; PP3D, Pinpoint 3D; BS, Beamscan Software; SRS, Stereotactic Radio Surgery

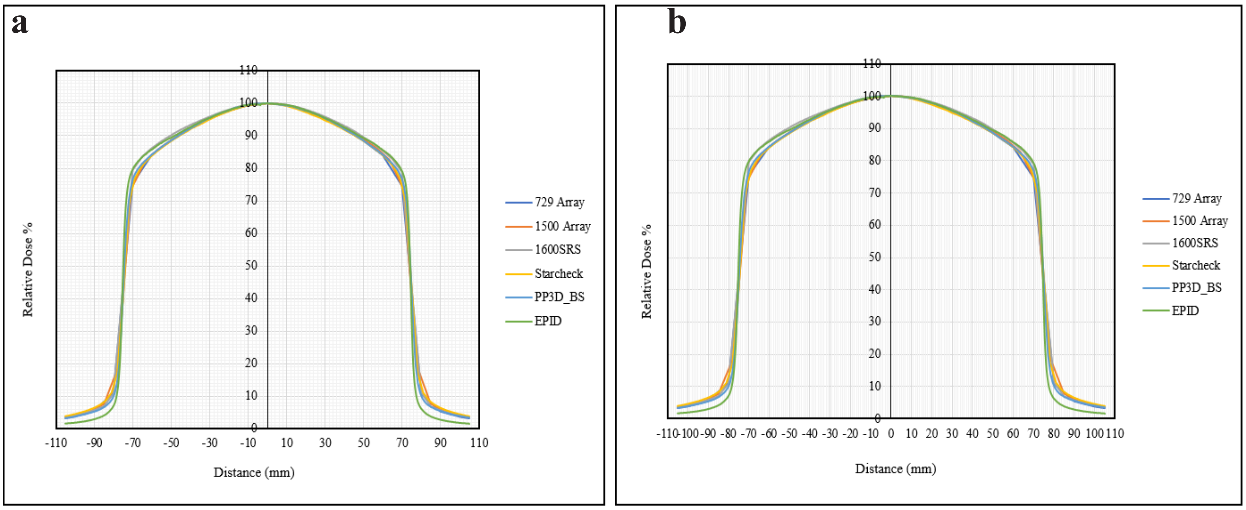

Figure 4. a, 6FFF_15X15 cm² Profiles; b, 10FFF_15X15 cm² Profiles. EPID, Electronic Portal Imaging Device; PP3D, Pinpoint 3D; BS, Beamscan Software; SRS, Stereotactic Radio Surgery

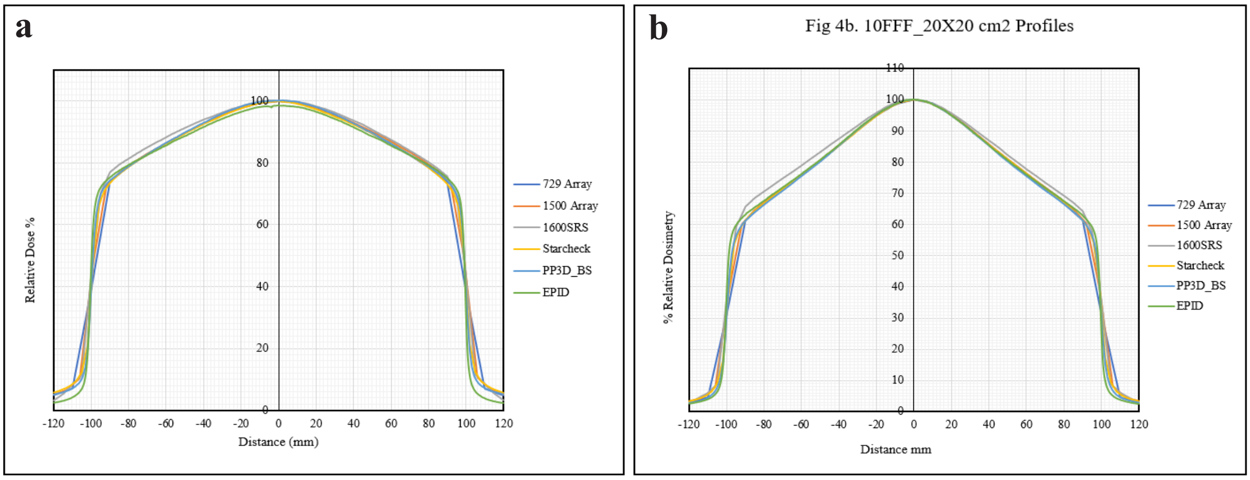

Figure 5. a. 6FFF_20X20 cm² Profiles; 5b. 10FFF_20X20 cm² Profiles. EPID, Electronic Portal Imaging Device; PP3D, Pinpoint 3D; BS, Beamscan Software; SRS, Stereotactic Radio Surgery

Table 4. Difference in (mm) FWHM between the Manual Analysis and the Software Analysis for 6FFF Beam.

	10X10 cm²	15X15 cm²	20X20 cm²
Array 729	5.16	0.09	3.40
Array 1500	4.07	0.05	3.54
Array 1600	4.06	1.33	2.83
Starcheck	0.72	0.33	1.55
PP3D	0.79	0.69	1.09
EPID	0.07	0.33	0.06

FWHM, Full Width Half Maximum; FFF, Flattening Filter Free; PP3D, Pinpoint 3D; EPID, Electronic Portal Imaging Device; mm, milli meter

Table 5. Difference in (mm) FWHM between the Manual Analysis and the Software Analysis for 10FFF Beam

	10X10 cm²	15X15 cm²	20X20 cm²
Array 729	5.02	0.14	4.66
Array 1500	3.78	0.05	3.55
Array 1600	2.03	2.26	2.69
Starcheck	0.67	0.25	1.75
Pinpoint 3D	0.39	0.15	0.24
EPID	0.16	0.05	0.18

FWHM, Full Width Half Maximum; FFF, Flattening Filter Free; PP3D, Pinpoint 3D; EPID, Electronic Portal Imaging Device; mm, milli meter

The 1,500 Array exhibited the second highest results. The resolution of these detector arrays caused this deviation. A discrepancy of less than 0.5 mm was noted among the measurements obtained by Pinpoint 3D, Starcheck, and EPID. Among all the detectors, it was observed that the EPID exhibited a higher degree of agreement with the software-generated data.

Discussion

Our findings and analysis proved that inflection points and field sizes were more accurate when a detector with a higher measurement resolution was exhibited. Additionally, it was noted that, with the exception of the Starcheck and EPID detector arrays, the effective built depths of the remaining arrays (729, 1,500, and 1,600) varied. As an illustration, chambers in 729 arrays were positioned at a distance of 7.5 mm; as a result, the actual radiation field in each chamber was not aligned. This factor contributed to the greater discrepancy between manual and software FWHM analyses for 10x10 cm^2 and 20x20 cm^2. Despite Starcheck's 3 mm resolution along the Primary and Diagonal axes of Field, which is in contrast to Pinpoint 3D's 1 mm and EPID's 0.3 mm, the inflection point is situated in close proximity to the measuring chambers. This produces FWHM that is comparable in precision to that of Pinpoint 3D and EPID detectors. The FWHM obtained with PinPoint 3D at a resolution of 1 mm was greater than 0.5 mm, with a maximal value of 1 mm observed. The discrepancy was notified to be less than 0.3 mm exclusively with EPID. According to Pichandi et al. [7], the 50% intensity level is observed in the steeply descending portion of the beam profile, which is a high gradient region. The field dimension of FFF beams deviates from the conventional definition. As Falk Ponisch et al. [33] and Fogliata et al. [12] already explained, the resolution of measurements constituted the sole cause of this discrepancy. The more the resolution, the lesser the variation in FWHM. However, the 15X15 cm^2 radiation field precisely intersected a chamber, causing the inflection point to be located there. The result was a negligible variation in FWHM. In contrast, a difference of greater than 2 mm was observed across all field diameters for a 1,600 array with a resolution of 5 mm for the 15X15 cm^2. At this location, the inflection point is absent at the chamber level. It is indisputable that the FWHM encountered distinctions because of detector resolution.

In conclusion, the results indicate that the detector's resolution has an impact on the inflection point and field width. The accuracy of identifying the inflection point increases as the resolution increases. While these detector arrays can be used to obtain consistent data for regular tests, this work emphasizes the need for high-resolution measurements, namely, at a minimum of 1 mm at a high gradient dose. Nevertheless, the inflection point determined through manual estimation aligns with the results obtained from program analysis solely in cases where the observed profile possesses a greater resolution. In addition, irrespective of the resolution of the detector, the software generates accurate measurements of the inflection point and field width. Ensuring enough resolution in the high gradient zone is of utmost importance when measuring the FFF beam profile. The efficacy of the PTW Software Module for Inflection Point Analysis has been found to be higher, rendering it suitable for routine quality assurance applications.

Author Contribution Statement

Kanakavel Kandasamy is responsible for conceptualization, Methodology, Software and Validation. Dr.James Jebaseelan Supervised the work.

Acknowledgements

Thanks to Mr. Boopalan, Dr. Imthiaz & Mr. Kumaravel of KLE Society and Hospital, Belgaum for their help and guidance in this project, and special gratitude & thanks to Mr. B. Viswanathan, PTW Dosimetry India Pvt Ltd. for providing radiation detector arrays for the study.

Potential Conflict of Interest

There is no mention of a conflict of interest.

Abbreviations

FFF: Flattening Filter Free
SRS & SBRT: Stereotactic Radio Surgery and Stereotactic Body Radiation Therapy
DMI: Digital Megavolt Imager
EPID: Electronic portal imaging device
PP3D: Pinpoint 3D Chamber
BS: Beam Scan
IAEA: International Atomic Energy Agency
IEC: International Electrotechnical Commission
SAD: Source-to-Axis Distance
FWHM: Full Width Half Maximum

References

1. Georg D, Knöös T, McClean B. Current status and future perspective of flattening filter free photon beams. Med Phys. 2011;38(3):1280-93. https://doi.org/10.1118/1.3554643.
2. Sharma SD. Unflattened photon beams from the standard flattening filter free accelerators for radiotherapy: Advantages, limitations and challenges. J Med Phys. 2011;36(3):123-5. https://doi.org/10.4103/0971-6203.83464.
3. Xiao Y, Kry SF, Popple R, Yorke E, Papanikolaou N, Stathakis S, et al. Flattening filter-free accelerators: A report from the aapm therapy emerging technology assessment work group. J Appl Clin Med Phys. 2015;16(3):5219. https://doi.org/10.1120/jacmp.v16i3.5219.
4. Masanga W, Tangboonduangjit P, Khamfongkhruea C, Tannanonta C. Determination of small field output factors in 6 and 10 mv flattening filter free photon beams using various detectors. J Phys: Conference Series. 2016;694:012027. https://doi.org/10.1088/1742-6596/694/1/012027.
5. Palmans H, Andreo P, Huq MS, Seuntjens J, Christaki K. Dosimetry of small static fields used in external beam radiotherapy: An iaea-aapm international code of practice for reference and relative dose determination. Vienna: International atomic energy agency. 2017 nov.
6. Sudhyadhom A, Kirby N, Faddegon B, Chuang CF. Technical note: Preferred dosimeter size and associated correction factors in commissioning high dose per pulse, flattening filter free x-ray beams. Med Phys. 2016;43(3):1507-13. https://doi.org/10.1118/1.4941691.
7. Pichandi A, Ganesh KM, Jerin A, Balaji K, Kilara G. Analysis of physical parameters and determination of inflection point for flattening filter free beams in medical linear accelerator. Rep Pract Oncol Radiother. 2014;19(5):322-31. https://doi.org/https://doi.org/10.1016/j.rpor.2014.01.004.
8. Shende R, Gupta G, Macherla S. Determination of an inflection point for a dosimetric analysis of unflattened beam using the first principle of derivatives by python code programming. Rep Pract Oncol Radiother. 2019;24(5):432-42. https://doi.org/10.1016/j.rpor.2019.07.009.
9. Choi MG, Law M, Yoon DK, Tamura M, Matsumoto K, Otsuka M, et al. Simplified sigmoidal curve fitting for a 6 mv fff photon beam of the halcyon to determine the field size for beam commissioning and quality assurance. Radiat Oncol. 2020;15(1):273. https://doi.org/10.1186/s13014-020-01709-x.

10. Muralidhar KR. Derivation of equations to define inflection point and its analysis in flattening filter free photon beams based on the principle of polynomial function. Int J Cancer Ther Oncol. 2015;3:1-5. https://doi.org/10.14319/ijcto.0301.5.
11. Fogliata A, Garcia R, Knoos T, Nicolini G, Clivio A, Vanetti E, et al. Definition of parameters for quality assurance of flattening filter free (fff) photon beams in radiation therapy. Med Phys. 2012;39(10):6455-64. https://doi.org/10.1118/1.4754799.
12. Sahani G, Sharma SD, Sharma PK, Deshpande DD, Negi PS, Sathianarayanan VK, et al. Acceptance criteria for flattening filter-free photon beam from standard medical electron linear accelerator: Aerb task group recommendations. J Med Phys. 2014;39(4):206-11. https://doi.org/10.4103/0971-6203.144482.
13. Hassan S, Deiab N, Aly A. A comparative study and dose evaluation of photon beam for water phantom, 2d-array and treatment planning system in small field sizes. Arab J Nucl Sci Appls. 2019:1-6. https://doi.org/10.21608/ajnsa.2019.13053.1217.
14. Ibrahim A, Mohamed I, Zidan H. Dosimetric comparison of amorphous silicon epid and 2d array detector for pre-treatment verification of intensity modulated radiation therapy. International Journal of Medical Physics, Clinical Engineering and Radiation Oncology. 2018;07:438-52. https://doi.org/10.4236/ijmpcero.2018.74037.
15. Decabooter E, Swinnen ACC, Öllers MC, Göpfert F, Verhaegen F. Operation and calibration of the novel ptw 1600srs detector for the verification of single isocenter stereotactic radiosurgery treatments of multiple small brain metastases. Br J Radiol. 2021; 94: 20210473. Https://doi.Org/10.1259/bjr.20210473.
16. Ibrahim S, Seshadri V, Charles P. Assessing the suitability of a two-dimensional array for routine quality assurance checks of flatness and symmetry. Phys Eng Sci Med. 2020;43(4):1451-60. https://doi.org/10.1007/s13246-020-00932-w.
17. Mhatre V, Pillakal S, Chadha P, Talapatra K. Dosimetric comparison of a-si 1200 and a-si 1000 electronic portal imager for intensity modulated radiation therapy (imrt). J Nucl Med Radiat Ther. 2018;09. https://doi.org/10.4172/2155-9619.1000354.
18. Varian manual "truebeam technical reference guide - volume 2: Imaging, p1005924-001-a" and epiqa version 4.1.1 is needed for dmi and truebeam 2.5. (december 2015): Available from: Https://www.Wienkav.At/kav/kfj/91033454/physik/tb/tb_dmi.Html.
19. Varian medical system (palo alto) cited on 21st april 2024 [internet]: Truebeam_productbrief_rad10128a_april2010.Pdf (widen.Net).
20. Ptw online catalogue for array detectors: D587.211.00/13 2024-01; page numbers: 18, 23, 24, 36, 37, 41 and 42 cited on 21st april 2024; downloads (ptwdosimetry.Com).
21. Ptw user manual for octavius detector 729: D913.131.00/06 en (november 2019) page number: 34.
22. Ptw online detector catalogue - d165.229.00/16 2023-12 quoted in page number 27; downloads (ptwdosimetry.Com).
23. Vieillevigne L, Arnaud F. Dosimetric performance of the new ptw 31022 pinpoint 3d ionization chamber in high energy photon beams. Biomed Phys Eng Express. 2018;4. https://doi.org/10.1088/2057-1976/aabeef.
24. Ptw rw3 slab phantom cited on 21st april 2024 [internet] rw3 slab phantom | ptw (ptwdosimetry.Com).
25. Verisoft software user manual d655.131.00/23 en © ptw-freiburg, 2021; page number 38.
26. Beamscan software user manual: D948.131.00/10 en, © ptw-freiburg, 2022 in appendix c in page number 556.
27. Andreo p, burns dt, hohlfeld k, huq m s, kanai t, laitano f, et al. Absorbed dose determination in external beam radiotherapy: An international code of practice for dosimetry based on standards of absorbed dose to water iaea technical report series no 398 international atomic energy agency, vienna 2000, https://doi.Org/10.61092/iaea.Ve7q-y94k.
28. Geneva: Iec; international electrotechnical commission, medical electrical equipment -medical electron accelerators -functional performance characteristics. 2007, iec 60976:2007 | iec webstore. Report no. Iec-60976. .
29. Gandhi A, Vellaiyan S, Subramanian VS, Shanmugam T, Murugesan K, Subramanian K. Commissioning of portal dosimetry using a novel method for flattening filter-free photon beam in a nontrue beam linear accelerator. J Cancer Res Ther. 2019;15(1):223-30. https://doi.org/10.4103/jcrt.JCRT_1181_16.
30. Calculus [internet] gilbert strang, massachusetts institute of technology "calculus" wellesley – cambridge press" [cited on 15th february 2024]: Available from: Calculus.Pdf (mit.Edu).
31. Ptw manual – beamscan software "analysis parameters for fff photon profiles" described in d948.131.00/09 and page no. 553.
32. Pönisch F, Titt U, Vassiliev ON, Kry SF, Mohan R. Properties of unflattened photon beams shaped by a multileaf collimator. Med Phys. 2006;33(6):1738-46. https://doi.org/10.1118/1.2201149.